

Designing enhanced entropy binding in single-chain nano particles

Lorenzo Rovigatti

*Department of Physics, Sapienza Università di Roma, Piazzale A. Moro 2, IT-00185 Roma, Italy and
CNR-ISC Uos Sapienza, Piazzale A. Moro 2, IT-00185 Roma, Italy*

Francesco Sciortino

*Department of Physics, Sapienza Università di Roma, Piazzale A. Moro 2, IT-00185 Roma, Italy
(Dated: July 26, 2022)*

Single-chain nanoparticles (SCNP) are a new class of bio and soft-matter polymeric objects in which a fraction of the monomers are able to form equivalently intra- or inter-polymer bonds. Here we numerically show that a fully-entropic gas-liquid phase separation can take place in SCNP systems. Control over the discontinuous (first-order) change — from a phase of independent diluted (fully-bonded) polymers to a phase in which polymers entropically bind to each other to form a (fully-bonded) polymer network — can be achieved by a judicious design of the patterns of reactive monomers along the polymer chain. Such a sensitivity arises from a delicate balance between the distinct entropic contributions controlling the binding.

Introduction: As elegantly epitomised in the van der Waals theory [1], in atomic systems the gas-liquid phase separation phenomenon originates from inter-particle attraction. More recently, colloidal systems have provided evidence of purely entropy-driven “gas-liquid” phase transitions, as observed in the presence of depletion interactions [2, 3], combinatorial attractions [4] and hard-core interactions between particles with specific shapes [5].

While depletion interactions have been studied in details in the last 30 years [3, 6], combinatorial attractions have received much less attention. In their seminal study, Safran and coworkers [4] investigated a system composed by microemulsion droplets linked by telechelic polymers [7]. The polymer body is exposed to the aqueous solvent while the hydrophobic ends are constrained to reside inside the same or in two distinct oil droplets. The different ways the polymer ends can be distributed over the accessible droplets leads to droplet condensation, i.e. to the liquid state. DNA-coated colloids provide further examples in which combinatorial entropy can be exploited to drive phase separation. Here particles are grafted with equal quantities of sticky ends and of their complementary sequence [8, 9], or grafted with palindromic sequences [10, 11]. In both cases, complete DNA hybridization can take place inside the same particle or between distinct particles and the balance between these two possibilities is controlled by a combinatorial entropic contribution.

In both telechelic polymers and DNA coated particles the dominant inter-particle contributions are strong interactions of the lock and key type such that the system is constantly in its energetic ground (fully-bonded) state. Particles can satisfy all possible bonds both in the gas phase (colloid poor) via intra-particle bonds as well as in the liquid phase (colloid rich), where bonds are shared between different particles. Being the number of bonds (and hence the energy) the same in both phases, entropy becomes the only driving force for condensation [12].

Functionalized polymers, in which a fraction of the monomers are able to form reversible bonds, have recently entered the radar of the soft-matter [13–21] and biophysics [22–26] communities, and experimentally synthesised even inside cells to promote gelation [27]. If the chain flexibility is large enough and the associative monomers can form only single bonds, then at low density bonding takes place essentially within the same polymer, forming soft nano-objects named single-chain nanoparticles (SCNP) [17]. At larger densities the combinatorial entropy should favour phase separation. However, in this case the free energy has additional terms that stem from the polymeric nature of the nanoparticles. Indeed, in contrast to colloids, where in addition to bonding the only other contribution is provided by the steric repulsion, in SCNP systems one has to also take into account the conformational entropy contribution associated to the change from an intra-polymer to an inter-polymer bond. The dependence of all these entropic terms on the number and type of attractive sites is complex [28] and has not been completely mapped out yet. In general, the interplay between the entropic contributions in play is subtle, and the resulting phase behaviour difficult to predict. In the specific case of SCNPs, at high density no hints of a first-order transition have been observed in experiments [18, 19] and simulations [29], consistent with predictions of mean-field theory [30]. By contrast, a continuous cross-over from isolated chains to percolating states have been observed [18, 19, 29], akin to the gelation without phase separation phenomenon observed in polymer and biopolymer systems [31, 32].

Here we show that, opposite to what previously found and thought, a fully-entropic gas-liquid phase separation can take place in SCNP systems. By studying a series of differently functionalized polymers we demonstrate that phase separation in this system takes place due to both the attractive combinatorial entropy and the conformational entropy contribution associated to the change from

an intra-polymer to an inter-polymer bond. We show that this last term can be modulated by designing the sequence of reactive monomers, offering the possibility to discontinuously change, preserving all bonds, from a dilute gas of independent polymers to a phase in which different polymers bind to each other to form an extended network.

We perform molecular dynamics simulations of Kremer-Grest polymers [33] complemented by attractive monomers that interact through a potential that enforces the single-bond per reactive monomer condition and enables a bond-swapping mechanism. The algorithm [34], recently applied to a variety of soft-matter systems [35–38], is capable to modify the bonding pattern close to the fully bonded state, even when the thermal energy $k_B T \equiv 1/\beta$ is much smaller than the bond strength ϵ_b , overcoming kinetic bottlenecks (see section S1).

We simulate polymers composed by $N_m = 254$ monomers, 24 of which are equispaced reactive and 230 inert. We study a model, named $(AAAA)_6$, in which all (A -type) reactive monomers are identical, a model in which A and B reactive monomers alternate, $(ABAB)_6$, and a model with four different (A, B, C, D) alternating reactive monomers, $(ABCD)_6$. A cartoon of the three studied polymer models is shown in Fig. 1(a-c). Reactive monomers are able to form one and only one strong bond with another same-type monomer. We perform two types of calculations. In the first, we simulate two polymers to compute the effective potential as a function of the relative distance between their centers of mass, while in the second one we perform bulk simulations of hundred or more polymers with periodic boundary conditions to compute the equation of state and the coexistence between phases. Further information on the numerical methods are available in Ref. [39].

The problem: Consider a SCNP, a polymer in which N_R of the constituent monomers are reactive. Each reactive monomer can form a strong bond with another reactive monomer of the same type on the same or on a nearby polymer. Different from functionalized colloidal (patchy) particles [40, 41], in which the rigidity of the particle prevents reactive monomers belonging to the same object from bonding with each other, in the polymer case all reactive monomers can take part in intra-polymer bonds. Being $\epsilon_b \gg k_B T$, each polymer can assume a fully bonded (ground state) configuration in which it is disconnected from all other polymers (Fig. 1(d-f)). This raises the question whether this “independent-polymer” state is the highest entropy state for a system of such polymers or if swapping intra-polymer for inter-polymer bonds can increase the system entropy even further. Even more important is the question about whether the increase in entropy, if present, is strong enough to induce condensation of a dense “liquid” phase starting from a dilute polymer solution.

Effective Potential (expectations): We begin in-

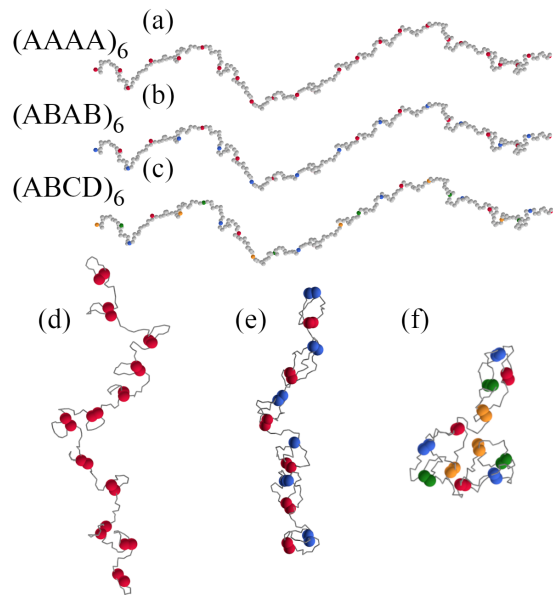


FIG. 1. Cartoons of the investigated polymers highlighting the different conformational changes associated to the formation of a fully bonded configuration in the three models considered. Here inert monomers are coloured in grey, while reactive monomers are depicted as coloured spheres. The three polymers are shown in an open, (a-c) and closed, (d-f), conformation. In (d-f) the inert monomers are not explicitly shown and the reactive monomers are shown with enhanced size for the sake of visibility.

vestigating the effective potential $\beta V_{\text{eff}}(R)$ between two polymers as a function of the relative center-to-center distance R , when $\epsilon_b \gg k_B T$. In this limit, the possible available configurations of two polymers are restricted to the ones in which all possible bonds are formed (either intra- or inter-polymer bonds). Being the total number of bonds always fixed, energy does not play any role in the interaction, leaving entropy as the only driving force. Three different entropic contributions determine $\beta V_{\text{eff}}(R)$. The first contribution includes the cost of bringing two fully-bonded polymers at relative distance R when only intra-polymer bonds are present. This is the standard polymer-polymer entropic repulsion [42–44]. The second contribution is a combinatorial term, which account for the entropy gain of swapping intra- with inter-polymer bonds. The number of configurations in which both intra and inter bonds are allowed is larger compared to the case in which only intra-polymer bonds are present (Section S4), resulting in an attractive contribution [11, 30].

The third and last contribution (S_{conf}) is linked to the conformational change of the polymer on going from the all intra-bond conformation to the mixed intra-/inter-bonds case. This entropic change accounts for the different number of configurations available to the inert monomers when the bonding pattern changes. S_{conf} is sensitive to the relative distances between identical reac-

tive monomers along the polymers and hence it can be tuned to control the strength of βV_{eff} by changing the types of the reactive monomers along the chain. Interestingly, as discussed in Section S2 simply changing the number of inert monomers while leaving the type and number of reactive monomers invariant does not modify the effective potential if distances are rescaled by the gyration radius.

Fig. 1(a-c) shows the three SCNP discussed here in an open configuration, while Fig. 1(d-e-f) shows the same models in a fully bonded configuration, to highlight the importance of the conformational entropic contribution. The figure vividly shows that on increasing the number of distinct reactive types, the fully bonded polymer becomes more compact. Assuming that bonds between nearest reactive monomers are the ones preferentially formed [30] (an hypothesis supported by simulations), to a first approximation each polymer in the bonded state can be visualised as an independent “unit” of paired reactive monomers, where the number of independent units is controlled by the number of reactive monomers of the same type. The change in conformational entropy $\Delta S_{\text{o} \rightarrow \text{fb}}$ of single chains going from an open unbonded state (identical for all polymers) to a fully bonded state (different for each of the three polymers considered) can be calculated *via* Hamiltonian integration (Sec. S1-F). The results, reported in Table I, confirm the progressive entropic cost of constraining the polymer into a configuration in which all bonds are formed on going from $(\text{AAAA})_6$ to $(\text{ABAB})_6$. Differences of about $1 k_B T$ per reactive monomer characterize the $(\text{ABAB})_6$ and the $(\text{ABCD})_6$ polymers as compared to the $(\text{AAAA})_6$ polymer, a significant configurational entropic cost required to satisfy all bond constraints, which can be partially regained when intra bonds are swapped with inter-polymer bonds.

Polymer type	$\Delta S_{\text{o} \rightarrow \text{fb}}/k_B$	$\Delta S_{\text{o} \rightarrow \text{fb}}/k_B$ per reactive site	R_g^2/σ^2
$(\text{AAAA})_6$	-93.0	-3.87	80
$(\text{ABAB})_6$	-110.6	-4.60	55
$(\text{ABCD})_6$	-119.3	-4.97	50

TABLE I. Entropy change $\Delta S_{\text{o} \rightarrow \text{fb}}/k_B$ from the open to the fully bonded state for the three polymer types. The error associated to $\Delta S_{\text{o} \rightarrow \text{fb}}/k_B$ is of the order of 10^{-1} . The last column reports the gyration radius R_g^2/σ^2 , where σ is the unit of length, corresponding to the monomer diameter.

Effective Potential (numerical evaluation): To evaluate the strength of the entropic contributions we compute (as described in Section S1-C) $\beta V_{\text{eff}}(R)$ for the three polymers. Note that we simulate under conditions that allow for bond breaking (such that the bond-swapping mechanism is active), but only configurations in which all possible bonds are formed are included in the statistical average. For each of the three models we

also evaluate the potential, $\beta V_{\text{eff}}^{\text{intra}}(R)$ where only intra-bonds are allowed. Results are shown in Fig. 2.

Consistent with mean-field theory [30] and recent simulations [45], in the $(\text{AAAA})_6$ case, despite the smaller $\beta V_{\text{eff}}^{\text{intra}}(R)$, $\beta V_{\text{eff}}(R)$ is always positive and close to zero for all R , indicating that there is no net attraction between the polymers: The entropic attraction almost completely compensates the entropic repulsion. Differently and strikingly, in the other two cases, $\beta V_{\text{eff}}(R)$ is strongly attractive, suggesting the possibility of a phase separation. Thus an appropriate design of the reactive monomer types can be used to control the resulting inter-polymer attraction. To confirm the enhanced inter-polymer binding, the inset of Fig. 2(b) shows the number of inter-polymer bonds for the three cases. In the $(\text{AAAA})_6$ case only a limited number of inter-polymer bonds are formed, even when the relative distance between the two polymers approaches zero. The conformational entropic gain of opening (two) intra-polymer bonds to form (two) inter-polymer bonds does not sufficiently compensate the entropic repulsion. The difference $\beta V_{\text{eff}}(R) - \beta V_{\text{eff}}^{\text{intra}}(R)$ provides a measure of the total entropic attraction between two polymers (sum of the combinatorial and of the conformational terms) and it is shown in Fig. 2(b). The contribution $\beta V_{\text{eff}}(R) - \beta V_{\text{eff}}^{\text{intra}}(R)$ for the $(\text{AAAA})_6$ and for the $(\text{ABAB})_6$ (and the $(\text{ABCD})_6$) sequences is quite different, confirming the different role played by entropy for the three polymer cases.

To support the numerical results for $\beta V_{\text{eff}}(R) - \beta V_{\text{eff}}^{\text{intra}}(R)$ we estimate the entropic attraction in an independent way. The partition function Z of the two-polymer system at fixed relative distance, when both intra and inter bonds are possible, can be approximated as a sum over the number of inter-polymer bonds $\#_b$ of a specific type, from 0 to the maximum number of bonds N_R :

$$Z = \sum_{\substack{0 \leq \#_b \leq N_R \\ \#_b \text{ even number}}} \Omega_{\#_b}. \quad (1)$$

The fully bonded condition imposes only even numbers for $\#_b$. Here $\Omega_{\#_b}$ counts the number of micro-states available to the two chains when $\#_b$ inter-bonds are present. The analogous expression, with the constraint of only intra-polymer bonds, would include only the first term of the sum ($\#_b = 0$) in Eq. 1. Hence the entropic loss $\Delta S/k_B$ on going from inter and intra bonds to only intra bonds is

$$\frac{\Delta S}{k_B} = \ln \frac{\Omega_0}{Z} \equiv \ln p(0), \quad (2)$$

The quantity $\ln p(0)$, which provides a neat (and independent) measure of the entropic attractive contribution, is

also reported in Fig. 2(b) and favourably compares with $\beta V_{\text{eff}}(R) - \beta V_{\text{eff}}^{\text{intra}}(R)$.

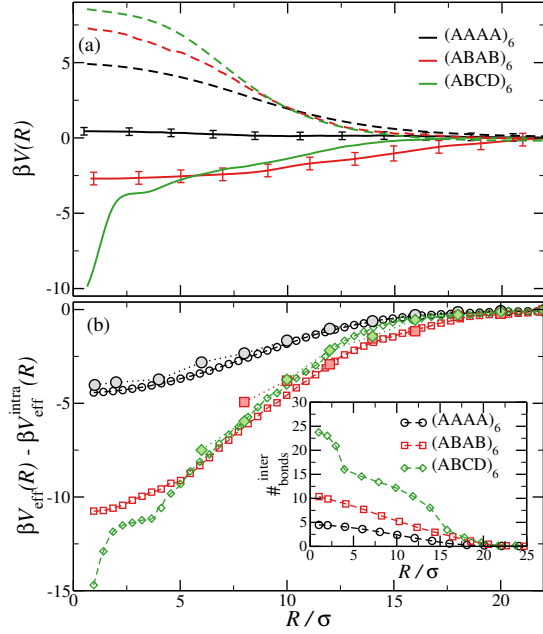


FIG. 2. (a) Effective potentials for the three polymers: $\beta V_{\text{eff}}(R)$ and $\beta V_{\text{eff}}^{\text{intra}}(R)$ are shown with solid and dashed lines, respectively. The error bars are upper bounds estimated by splitting the data in two blocks and computing the absolute difference between the effective interactions in each block, divided by $\sqrt{2}$. (b) Attractive part of the potential estimated as $\beta V_{\text{eff}}(R) - \beta V_{\text{eff}}^{\text{intra}}(R)$ (open symbols) and as $\ln p(0)$ (see Eq. 2, filled symbols). The inset shows the average number of inter-polymer bonds. Note that the abrupt decrease of $\beta V_{\text{eff}}(R)$ for very short R in the (ABCD)₆ case originates from *zipping* of the bonds.

In Section S2 we show that the observed trends are robust for changes in the polymer length (at fixed number of reactive monomers, by increasing the number of inert monomers) as well as for changes at fixed polymer length on changing the number of reactive monomers.

Phase Behavior: To confirm that the entropic attraction for the (ABAB)₆ and (ABCD)₆ polymers is sufficiently strong to condensate a “liquid” from the “gas”, we evaluate their equation of state (Fig. 3(a)), calculated as discussed in Section S1-D. Coherently with the two-body effective interaction results, the (AAAA)₆ system behaves essentially as an ideal gas. Interestingly, this θ -condition originates from the ability of the entropic attraction to essentially compensate the usual polymer repulsion. By contrast, the pressure in both the (ABAB)₆ and (ABCD)₆ systems becomes quickly negative, suggesting the presence of a phase transition between two phases with significantly different polymer concentration. As a proof of the possible presence of a phase separation we perform direct-coexistence simulations (Section S1-E), by preparing a starting configuration composed by an inhomogeneous polymer concentration. Fig. 3(b) shows

the density profiles of the initial and final configurations for all three models. The density of the (AAAA)₆ system becomes homogeneous and the two interfaces that were present at time zero completely disappear. By contrast, the gas-liquid interfaces are stable in both the (ABAB)₆ and (ABCD)₆ systems over the course of the simulation. We find (not shown) that in the liquid phase at coexistence the system percolates and that each polymer binds with ≈ 10 other polymers for the (ABAB)₆ and (ABCD)₆ models.

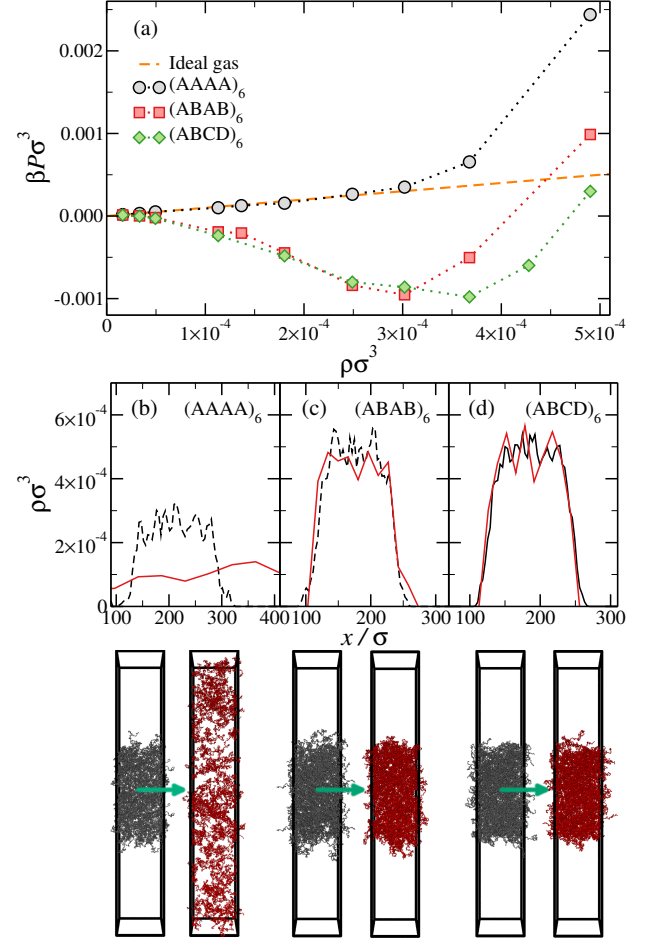


FIG. 3. (a) Equations of state of the three investigated systems (points) and of an ideal gas of chains (orange dashed line). The statistical uncertainty is smaller than the symbol size. (b-d) Density profiles along x for the three investigated systems evaluated with direct coexistence simulations. We show the profiles of the density of the initial configuration (dashed black lines) and of the average density of the final state (solid red lines). Representative snapshots of the initial (grey) and final (red) states are shown below each plot.

Concluding Remarks: In summary, we have demonstrated that opposite to what previously expected, a gas-liquid phase separation can appear in systems of SC-NPs. By simply alternating two different types of reactive monomers, it is possible to tune the conformational entropy change on swapping intra to inter binding. As a

result, the strength of configurational and combinatorial entropy can be harnessed to induce a fully entropic first-order phase transition, even with a low overall concentration of reactive monomers. In view of the modern ability to force living cells to express SCNP, it is foreseeable to imagine — guided by entropy — a fine tuned control of the phase behavior of these particles in biologically relevant conditions [27] as well as a mechanism to optimise multivalent binding [46, 47] in ligand-receptors equilibria. At the same time, the design principles reported here may help achieving a better understanding of phase separation phenomena in cells, which are most often mediated by multivalent biomacromolecules [48–50]. Such phenomena are commonly termed “liquid-liquid” transitions, since in both phases proteins are dispersed in an aqueous solvent — the protein rich and poor phases being respectively the liquid and the gas in the present (implicit solvent) model.

Acknowledgement: We acknowledge support from MIUR PRIN 2017 (Project 2017Z55KCW) and the CINECA award under the ISCRA initiative, for the availability of high performance computing resources and support (Iskra B "AssoPoN"). We thank Angel Moreno for fruitful discussions.

-
- [1] Van der Waals, Ph.D. thesis, University of Leiden (1873).
 - [2] Sho Asakura and Fumio Oosawa, “On interaction between two bodies immersed in a solution of macromolecules,” *The Journal of Chemical Physics* **22**, 1255–1256 (1954).
 - [3] Remco Tuinier and Henk NW Lekkerkerker, *Colloids and the depletion interaction* (Springer Netherlands, 2011).
 - [4] A Zilman, J Kieffer, F Molino, G Porte, and SA Safran, “Entropic phase separation in polymer-microemulsion networks,” *Physical review letters* **91**, 015901 (2003).
 - [5] Sangmin Lee, Erin G Teich, Michael Engel, and Sharon C Glotzer, “Entropic colloidal crystallization pathways via fluid-fluid transitions and multidimensional prenucleation motifs,” *Proceedings of the National Academy of Sciences* **116**, 14843–14851 (2019).
 - [6] Fumio Oosawa, “The history of the birth of the asakura-oosawa theory,” *J. Chem. Phys.* **155**, 084104 (2021).
 - [7] Mohammed Filali, Mohamed Jamil Ouazzani, Eric Michel, Raymond Aznar, Grégoire Porte, and Jacqueline Appell, “Robust phase behavior of model transient networks,” *The Journal of Physical Chemistry B* **105**, 10528–10535 (2001).
 - [8] Stefano Angioletti-Uberti, Bortolo M Mognetti, and Daan Frenkel, “Re-entrant melting as a design principle for dna-coated colloids,” *Nature materials* **11**, 518–522 (2012).
 - [9] Stephan Jan Bachmann, Jurij Kotar, Lucia Parolini, Andela Šarić, Pietro Cicuta, Lorenzo Di Michele, and Bortolo Matteo Mognetti, “Melting transition in lipid vesicles functionalised by mobile dna linkers,” *Soft Matter* **12**, 7804–7817 (2016).
 - [10] Francesco Sciortino, “Entropy in self-assembly,” *La Rivista del Nuovo Cimento* **42**, 511–548 (2019).
 - [11] Francesco Sciortino, Yugang Zhang, Oleg Gang, and Sanat K Kumar, “Combinatorial-entropy-driven aggregation in dna-grafted nanoparticles,” *ACS nano* **14**, 5628–5635 (2020).
 - [12] Frank Smallenburg and Francesco Sciortino, “Liquids more stable than crystals in particles with limited valence and flexible bonds,” *Nature Physics* **9**, 554–558 (2013).
 - [13] Sanat K Kumar and Jack F Douglas, “Gelation in physically associating polymer solutions,” *Physical review letters* **87**, 188301 (2001).
 - [14] Myungeun Seo, Benjamin J Beck, Jos MJ Paulusse, Craig J Hawker, and Sang Youl Kim, “Polymeric nanoparticles via noncovalent cross-linking of linear chains,” *Macromolecules* **41**, 6413–6418 (2008).
 - [15] Christopher K Lyon, Alka Prasher, Ashley M Hanlon, Bryan T Tuten, Christian A Tooley, Peter G Frank, and Erik B Berda, “A brief user’s guide to single-chain nanoparticles,” *Polymer Chemistry* **6**, 181–197 (2015).
 - [16] Arantxa Arbe, José A Pomposo, Angel J Moreno, F LoVerso, M González-Burgos, I Asenjo-Sanz, A Iturrospe, A Radulescu, O Ivanova, and J Colmenero, “Structure and dynamics of single-chain nano-particles in solution,” *Polymer* **105**, 532–544 (2016).
 - [17] José A Pomposo, *Single-Chain Polymer Nanoparticles: Synthesis, Characterization, Simulations, and Applications* (John Wiley & Sons, 2017).
 - [18] Daniel E Whitaker, Clare S Mahon, and David A Fulton, “Thermoresponsive dynamic covalent single-chain polymer nanoparticles reversibly transform into a hydrogel,” *Angewandte Chemie* **125**, 990–993 (2013).
 - [19] Shengchang Tang, Muzhou Wang, and Bradley D Olsen, “Anomalous self-diffusion and sticky rouse dynamics in associative protein hydrogels,” *Journal of the American Chemical Society* **137**, 3946–3957 (2015).
 - [20] Ashesh Ghosh and Kenneth S Schweizer, “Physical bond breaking in associating copolymer liquids,” *ACS Macro Letters* **10**, 122–128 (2020).
 - [21] Bernardo Oyarzún and Bortolo Matteo Mognetti, “Programming configurational changes in systems of functionalised polymers using reversible intramolecular linkages,” *Molecular Physics* **116**, 2927–2941 (2018).
 - [22] Antonia Statt, Helena Casademunt, Clifford P Brangwynne, and Athanassios Z Panagiotopoulos, “Model for disordered proteins with strongly sequence-dependent liquid phase behavior,” *The Journal of chemical physics* **152**, 075101 (2020).
 - [23] Kiersten M Ruff, Furqan Dar, and Rohit V Pappu, “Ligand effects on phase separation of multivalent macromolecules,” *Proceedings of the National Academy of Sciences* **118** (2021).
 - [24] Simon M Lichtinger, Adiran Garaizar, Rosana Collepardo-Guevara, and Aleks Reinhardt, “Targeted modulation of protein liquid-liquid phase separation by evolution of amino-acid sequence,” *PLOS Computational Biology* **17**, e1009328 (2021).
 - [25] Gregory L Dignon, Wenwei Zheng, Robert B Best, Young C Kim, and Jeetain Mittal, “Relation between single-molecule properties and phase behavior of intrinsically disordered proteins,” *Proceedings of the National Academy of Sciences* **115**, 9929–9934 (2018).
 - [26] Emiko Zumbro, Jacob Witten, and Alfredo Alexander-Katz, “Computational insights into avidity of polymeric

- multivalent binders,” *Biophysical Journal* **117**, 892–902 (2019).
- [27] Hideki Nakamura, Albert A Lee, Ali Sobhi Afshar, Shigeki Watanabe, Elmer Rho, Shiva Razavi, Allister Suarez, Yu-Chun Lin, Makoto Tanigawa, Brian Huang, *et al.*, “Intracellular production of hydrogels and synthetic rna granules by multivalent molecular interactions,” *Nature materials* **17**, 79–89 (2018).
- [28] Angel J Moreno, Petra Bacova, Federica Lo Verso, Arantxa Arbe, Juan Colmenero, and José A Pomposo, “Effect of chain stiffness on the structure of single-chain polymer nanoparticles,” *Journal of Physics: Condensed Matter* **30**, 034001 (2017).
- [29] Maud Formanek, Lorenzo Rovigatti, Emanuela Zaccarelli, Francesco Sciortino, and Angel J Moreno, “Gel formation in reversibly cross-linking polymers,” *Macromolecules* **54**, 6613–6627 (2021).
- [30] Alexander N Semenov and Michael Rubinstein, “Thermoreversible gelation in solutions of associative polymers. 1. statics,” *Macromolecules* **31**, 1373–1385 (1998).
- [31] Paul J Flory, “Constitution of three-dimensional polymers and the theory of gelation,” *The Journal of Physical Chemistry* **46**, 132–140 (1942).
- [32] Tyler S Harmon, Alex S Holehouse, Michael K Rosen, and Rohit V Pappu, “Intrinsically disordered linkers determine the interplay between phase separation and gelation in multivalent proteins,” *elife* **6**, e30294 (2017).
- [33] Kurt Kremer and Gary S Grest, “Dynamics of entangled linear polymer melts: A molecular-dynamics simulation,” *The Journal of Chemical Physics* **92**, 5057–5086 (1990).
- [34] Francesco Sciortino, “Three-body potential for simulating bond swaps in molecular dynamics,” *The European Physical Journal E* **40**, 3 (2017).
- [35] Nicoletta Gnan, Lorenzo Rovigatti, Maxime Bergman, and Emanuela Zaccarelli, “In silico synthesis of microgel particles,” *Macromolecules* **50**, 8777–8786 (2017).
- [36] Lorenzo Rovigatti, Giovanni Nava, Tommaso Bellini, and Francesco Sciortino, “Self-dynamics and collective swap-driven dynamics in a particle model for vitrimers,” *Macromolecules* **51**, 1232–1241 (2018).
- [37] Simone Ciarella, Francesco Sciortino, and Wouter G Ellenbroek, “Dynamics of vitrimers: Defects as a highway to stress relaxation,” *Physical review letters* **121**, 058003 (2018).
- [38] Valerio Sorichetti, Andrea Ninarello, José M Ruiz-Franco, Virginie Hugouvieux, Walter Kob, Emanuela Zaccarelli, and Lorenzo Rovigatti, “Effect of chain polydispersity on the elasticity of disordered polymer networks,” *Macromolecules* **54**, 3769–3779 (2021).
- [39] “See supplemental material at <http://link.aps.org/supplemental/xxxx/xxxx> for a detailed description of the methods and for results about additional polymers, including refs. [51–54],”.
- [40] Emanuela Bianchi, Julio Largo, Piero Tartaglia, Emanuela Zaccarelli, and Francesco Sciortino, “Phase diagram of patchy colloids: Towards empty liquids,” *Physical Review Letters* **97**, 168301 (2006).
- [41] Francesco Sciortino and Emanuela Zaccarelli, “Equilibrium gels of limited valence colloids,” *Current opinion in colloid & interface science* **30**, 90–96 (2017).
- [42] Alexander Yu Grosberg, Pavel G Khalatur, and Alexei R Khokhlov, “Polymeric coils with excluded volume in dilute solution: The invalidity of the model of impenetrable spheres and the influence of excluded volume on the rates of diffusion-controlled intermacromolecular reactions,” *Die Makromolekulare Chemie, Rapid Communications* **3**, 709–713 (1982).
- [43] PG Bolhuis, AA Louis, JP Hansen, and EJ Meijer, “Accurate effective pair potentials for polymer solutions,” *The Journal of Chemical Physics* **114**, 4296–4311 (2001).
- [44] Christos N Likos, “Effective interactions in soft condensed matter physics,” *Physics Reports* **348**, 267–439 (2001).
- [45] Mariarita Paciolla, Christos N Likos, and Angel J Moreno, “On the validity of effective potentials in crowded solutions of linear and ring polymers with reversible bonds,” *arXiv preprint arXiv:2112.13067* (2021).
- [46] Galina V Dubacheva, Tine Curk, Bortolo M Moggetti, Rachel Auzély-Velty, Daan Frenkel, and Ralf P Richter, “Superselective targeting using multivalent polymers,” *Journal of the American Chemical Society* **136**, 1722–1725 (2014).
- [47] Meng Liu, Azzurra Apriceno, Miguel Sipin, Edoardo Scarpa, Laura Rodriguez-Arco, Alessandro Poma, Gabriele Marchello, Giuseppe Battaglia, and Stefano Angioletti-Uberti, “Combinatorial entropy behaviour leads to range selective binding in ligand-receptor interactions,” *Nature communications* **11**, 1–10 (2020).
- [48] Anthony A Hyman, Christoph A Weber, and Frank Jülicher, “Liquid-liquid phase separation in biology,” *Annual review of cell and developmental biology* **30**, 39–58 (2014).
- [49] Clifford P Brangwynne, Peter Tompa, and Rohit V Pappu, “Polymer physics of intracellular phase transitions,” *Nature Physics* **11**, 899–904 (2015).
- [50] Salman F Banani, Hyun O Lee, Anthony A Hyman, and Michael K Rosen, “Biomolecular condensates: organizers of cellular biochemistry,” *Nature reviews Molecular cell biology* **18**, 285–298 (2017).
- [51] Frank H Stillinger and Thomas A Weber, “Computer simulation of local order in condensed phases of silicon,” *Physical review B* **31**, 5262 (1985).
- [52] Alan M Ferrenberg and Robert H Swendsen, “Optimized monte carlo data analysis,” *Computers in Physics* **3**, 101–104 (1989).
- [53] John Russo, Piero Tartaglia, and Francesco Sciortino, “Reversible gels of patchy particles: role of the valence,” *The Journal of Chemical Physics* **131**, 014504 (2009).
- [54] Maud Formanek and Angel J Moreno, “Effects of precursor topology and synthesis under crowding conditions on the structure of single-chain polymer nanoparticles,” *Soft Matter* **13**, 6430–6438 (2017).

Supplementary Information to “Designing enhanced entropy binding in single-chain nano particles”

Lorenzo Rovigatti and Francesco Sciortino

Department of Physics, Sapienza Università di Roma, Piazzale A. Moro 2, IT-00185 Roma, Italy

(Dated: July 26, 2022)

S1. MODELS AND NUMERICAL DETAILS

A. Models

In the main text we discuss three polymer models. Each polymer is composed by $N_m = 254$ monomers (24 reactive and 230 inert monomers M). Reactive monomers are equally spaced by ten inert monomers each. The 24 reactive monomers can be of four types, which we label A, B and C and D. The first polymer ((AAAA)₆ in the following) is composed only of A-type reactive monomers. The second polymer ((ABAB)₆ in the following) is composed by an alternate regular sequence of A-type and B-type reactive monomers. Finally, the third polymer ((ABCD)₆ in the following) is composed by an alternate regular sequence of A-B- C- and D-type reactive monomers. The sequences are reported in Table S1 and pictorially represented in the snapshots of the main text.

Name	Sequence
(AAAA) ₆	(AM ₁₀) ₂₃ A
(ABAB) ₆	(AM ₁₀ BM ₁₀) ₁₁ AM ₁₀ B
(ABCD) ₆	(AM ₁₀ BM ₁₀ CM ₁₀ DM ₁₀) ₅ AM ₁₀ BM ₁₀ CM ₁₀ D

TABLE S1. The three main polymers investigated in this work.

B. Numerical Details: interaction potential

All monomers that are nearest-neighbours along the chain (topologically bonded) interact through the Kremer-Grest [1] force field, sum of a WCA potential and a FENE potential. More precisely, defining r as the distance between bonded monomers,

$$V_{\text{WCA}}(r) = 4\epsilon \left[\left(\frac{r}{\sigma} \right)^{12} - \left(\frac{r}{\sigma} \right)^6 \right] + V_{\text{shift}} \quad r < 2^{1/6} \quad (\text{S1})$$

where ϵ and σ are the units of energy and length respectively and V_{shift} is a constant that brings V_{WCA} to zero at $r = 2^{1/6}\sigma$. For $r > 2^{1/6}\sigma$ $V_{\text{WCA}}(r) = 0$. The FENE potential is

$$V_{\text{FENE}}(r) = -\frac{1}{2}Kd_0^2 \ln \left(1 - \frac{d_0}{r} \right)^2 \quad (\text{S2})$$

where $d_0 = 1.5\sigma$ and $K = 30\epsilon/\sigma^2$. Non-bonded monomers interacts via an excluded-volume interaction,

modeled with the same WCA potential. The only attractive contribution arises from the interaction between the reactive monomers.

To model binding, we borrow a functional form proposed by Stillinger and Weber [2] in their model for Silicon. The corresponding interaction potential $V_{\text{bind}}(R)$ is

$$V_{\text{bind}}(r) = A\epsilon_b \left[B \left(\frac{\sigma_s}{r} \right)^4 - 1 \right] e^{\sigma_s/(r-r_c)} \quad (\text{S3})$$

where $\sigma_s = 1.05\sigma$, $r_c = 1.68\sigma$, $B = 0.41$, $A = 8.97$. The coefficient ϵ_b modulates the strength of the binding attraction. V_{bind} goes continuously to zero as r approaches r_c . In what follows, the attractive potential acts only between reactive monomers of the same type.

To enforce the single-bond per reactive monomer condition we implement a repulsive three body interaction V_{3b} which penalizes the formation of triplets of bonded monomers [3]. In addition, V_{3b} is designed to almost exactly compensate the gain associated to the formation of a second bond, originating an almost flat energy hypersurface which favours bond swapping even in the presence of pair attraction energies much larger than the thermal energy. The V_{3b} interaction potential reads

$$V_{3b}(r_{ij}, r_{ik}) = 0.9\epsilon_b \sum_{ijk} V_3(r_{ij})V_3(r_{ik}) \quad (\text{S4})$$

where the sum runs over all triplets of bonded particles (monomer i bonded both with k and j). r_{ij} is the distance between particle i and j . The pair potential $V_3(r)$ is defined in terms of the normalized $V_{\text{bind}}(r)$ as

$$V_3(r) = \left\{ \begin{array}{ll} 1 & r \leq r_{\min} \\ -\frac{V_{\text{bind}}(r)}{\epsilon_b}, & r_{\min} \leq r \leq r_c \end{array} \right\} \quad (\text{S5})$$

where r_{\min} is the distance at which $V_{\text{bind}}(r)$ has a minimum. We note on passing that no additional computational resources are requested to calculate $V_{3b}(r_{ij}, r_{ik})$, since the latter is defined in terms of previously calculated quantities. We also note that differently from the Stillinger-Weber potential [2], which favours the formation of a tetrahedral ordering via an angular dependence, here the three-body potential does not depend on r_{jk} .

Fig. S1 shows the shape of V_{WCA} (Eq. S1), $V_{\text{bind}}(r)$ (Eq. S3), and $V_3(r)$ (Eq.S5).

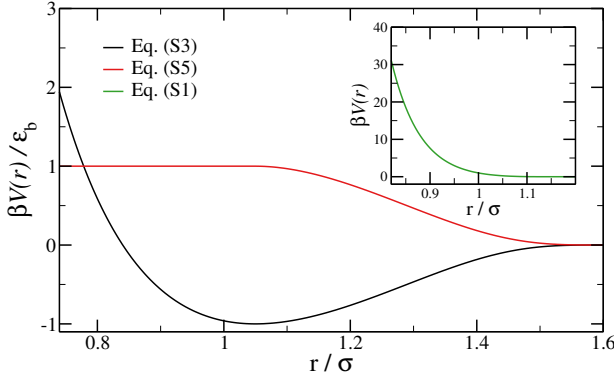


FIG. S1. The different potentials acting between non-bonded monomers.

C. Numerical Details: Effective potential calculations

We have calculated the effective potential performing simulations of two identical polymers at $k_B T = 1$ for $12 < \epsilon_b < 17$ constrained by a harmonic potential acting on the relative distance R between their centres of mass $R \equiv |\vec{r}_1^{CM} - \vec{r}_2^{CM}|$ and centred around R_0 ,

$$V_{\text{umbrella}}(R) = \frac{1}{2} K (R - R_0)^2 \quad (\text{S6})$$

We have explored 15 different R_0 values, spaced from $R_0 = \sigma$ to $R_0 = 30\sigma$. For each simulation i we have computed the probability distribution $P(R)$ that the two centres of mass are at a distance R .

From $P(R)$ the effective potential $\beta V_{\text{eff}}(R)$ can be estimated as

$$\beta V_{\text{eff}}(R) \sim -\ln \left(\frac{P(R)}{R^2} e^{\beta V_{\text{umbrella}}(R)} \right) \quad (\text{S7})$$

We extract from the simulation the configurations in which all possible bonds are formed. Only these configurations are included in the statistical average. The top panel of Figure S2 shows how the bonding pattern evolves during a simulation for the $R = 10\sigma$ window of the AAAA polymer: the number of bonds fluctuate and fully-bonded configurations are obtained repeatedly. By extracting the fully-bonded configurations it is possible to follow the time evolution of the inter-polymers bonds (green dots), in fully bonded states. Similar results are obtained for all investigated center of mass distances and for all polymer models.

The bottom panel of Figure S2 shows the bond autocorrelation function, defined as the probability that a bond that is present at $t = 0$ also exists, without ever being broken, at a later time t , as computed for selected umbrella sampling windows in the whole range of explored chain-chain separations for the ABCD system, which is the system with the slowest convergence rate of all the systems. For all explored windows, the probability that

a bond exists uninterruptedly for $\approx 8 \times 10^6 \sigma \sqrt{m/\epsilon}$ is always less than 10^{-7} . We note that our simulations run for at least four times longer than the time range shown here, meaning that the system is able to completely forget about its initial bonding pattern several times during the course of the simulation.

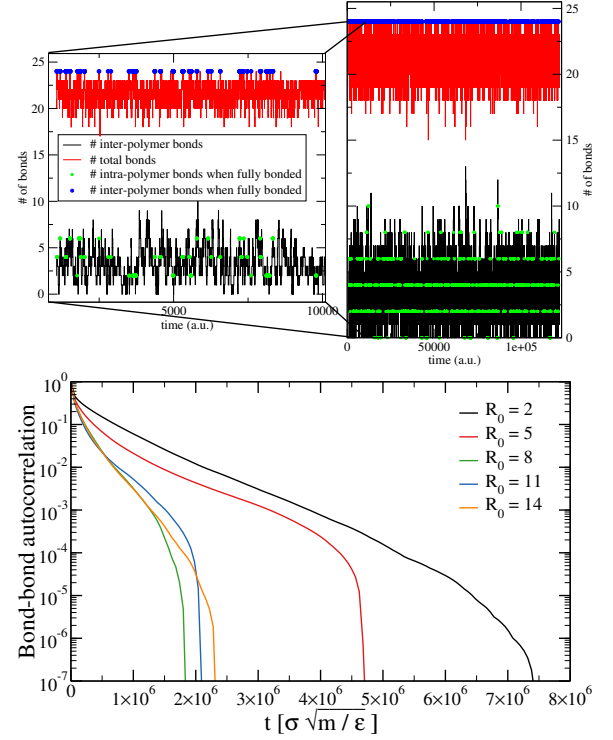


FIG. S2. Top: Time dependence of the total number of bonds (intra and inter) and of the intra bonds for two AAAA polymers fixed at center of mass distance 10σ when $\beta\epsilon_b = 13$. The left panel is a zoom-in of the right panel that highlights the evolution of the time series. Bottom: The bond autocorrelation function for the ABCD system for selected umbrella sampling windows. Note that the overall length of the simulations is roughly four times longer than the time interval shown here ($\approx 3.2 \times 10^7 \sigma \sqrt{m/\epsilon}$).

For each of the three models we evaluated two effective interactions: the full potential, $V_{\text{eff}}(R)$, and the potential between polymers that can bind only intramolecularly, $V_{\text{eff}}^{\text{intra}}(R)$. In this latter case the calculated potential provides a measure of the repulsive excluded volume contribution. The difference $V_{\text{eff}}(R) - V_{\text{eff}}^{\text{intra}}(R)$ provides a measure of the entropic attraction between the two polymers. This entropic contribution is the sum of the combinatorial and conformational terms.

Result from different simulations have been combined together with the WHAM method [4].

D. Numerical Details: Equation of state calculations

For the (AAAA)₆, (ABAB)₆ and (ABCD)₆ models we have run bulk molecular dynamics simulations at constant volume V , temperature T and number of polymers N_c . We use a velocity Verlet integrator with time step $\delta t = 0.003$ in units of $\sigma\sqrt{m/\epsilon}$, where m is the mass of a monomer, and a Andersen-like thermostat [5]. We fix $k_B T = 1$, $N_c = 100$ and vary V to compute the equation of state in the required density range.

E. Numerical Details: Direct coexistence calculations

We have also performed direct-coexistence molecular dynamics simulations in which we use an elongated box size along the x axis containing $N_c = 200$ chains. We use the same simulation parameters of Section S1 D.

Since each reactive monomer can be involved in a single bond only, the maximum number of bonds that can be formed is given by $N_b^{\max} = 24N_c/2$. We define $p_b = N_b/N_b^{\max}$, where N_b is the number of formed bonds. In the simulations there are never more than 2 unformed bonds (*i.e.* $p_b > 0.993$), so that we can safely assume that the energy is constant and the only driving force is entropic.

F. Numerical Details: Hamiltonian integration

We evaluate the entropy difference $\Delta S_{o \rightarrow fb}$ between the open and fully-bonded state for the (AAAA)₆, (ABAB)₆ and (ABCD)₆ SCNP. To do so we run several simulations of single polymers at 21 equally spaced values of the binding strength ϵ_b ranging from $\epsilon_b = 0$, which corresponds to an open state (identical for all polymers), to $\epsilon_b = 20$, corresponding to a fully bonded state (different for all polymer types). The change in free energy between the two states is given by

$$\Delta F_{o \rightarrow fb} = \int_0^{20} \left\langle \frac{U_b}{\epsilon_b} \right\rangle d\epsilon_b \quad (S8)$$

where U_b is the total binding energy of a configuration and $\langle \cdot \rangle$ is an ensemble average. Since, by definition, $\Delta F_{o \rightarrow fb} = \Delta U_{o \rightarrow fb} - T\Delta S_{o \rightarrow fb}$, where $\Delta U_{o \rightarrow fb}$ is the difference in the average total energy between the two states, the entropy difference between the open and closed state of a given polymer is

$$\Delta S_{o \rightarrow fb} = \frac{\Delta U_{o \rightarrow fb} - \Delta F_{o \rightarrow fb}}{T}. \quad (S9)$$

Figure S3 shows $\left\langle \frac{U_b}{\epsilon_b} \right\rangle$ and $\Delta S_{o \rightarrow fb}$ for the three polymer models investigated in the main text.

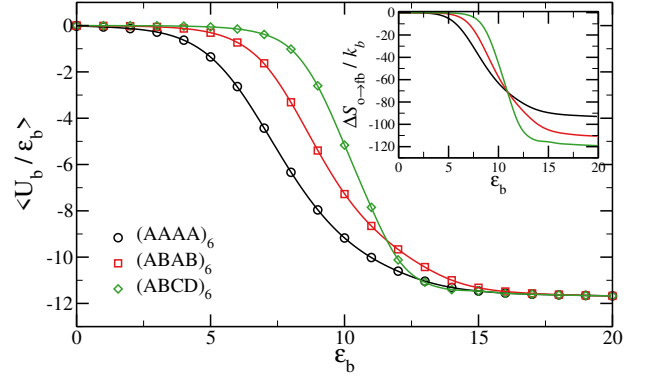


FIG. S3. The integrand of Eq. S8 as a function of the two-body interaction strength ϵ_b for the three polymer models studied in the main text. The inset shows the resulting entropy difference computed through Eq. S9.

S2. ADDITIONAL POLYMERS

A. Varying the spacing between the reactive sites

We evaluate here the effect of the spacing between reactive sites by comparing the same three polymers studied in the article with three additional polymers with the very same number of reactive sites (24), but spaced by $M = 20$ inert monomers (instead of $M = 10$). The total length of these additional three polymers is thus $N_m = 484$ monomers (24 reactive and 460 inert monomers M). The gyration radius of the three new polymers is reported in Table S2.

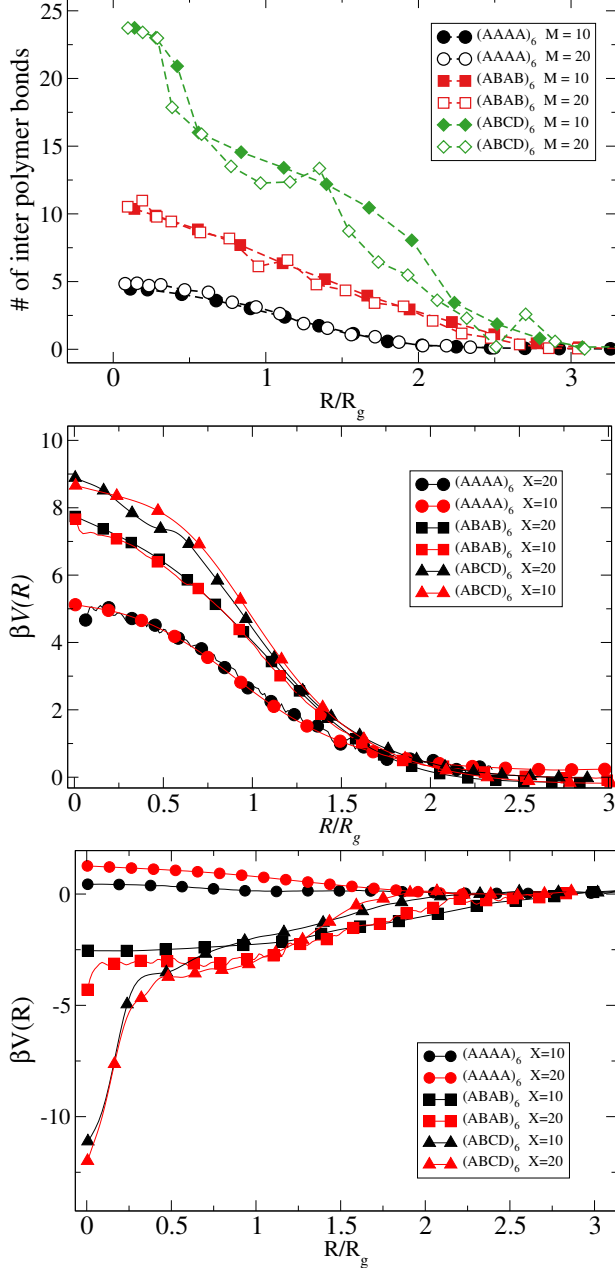
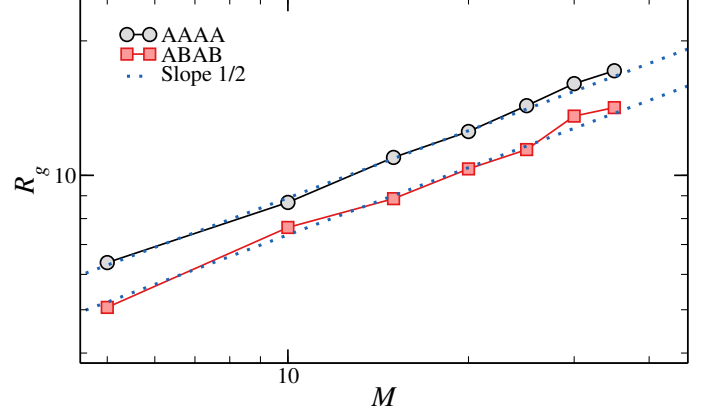
Figure S4 shows that, when plotted as a function of R/R_g , the number of inter-polymer bonds, the only-intra potential and the effective potential, are seemingly independent (or weakly dependent) of M .

Data on irreversible single-chain nanoparticles show that the scaling exponents of irreversible fully-flexible SCNPs are those of Gaussian chains [6, 7]. Figure S5 shows that this is the case also for fully-bonded, reversible SCNPs, as the dependence of the radius of gyration of both AAAA and ABAB polymers on M is compatible with an exponent 0.5. Data of Ref. [6] also shows that the gyration radius of the loops (which is related to the entropic cost of forming a loop) scales with M with apparent exponents that depend on the loop size. As a result, understanding the reason for the weak M dependence is not straightforward and simple scaling (mean-field-like) arguments like those of Ref. [8] need a finer tuning.

Regardless of its origin, the consequence on the thermodynamics of this scaling can be stated by saying that the phase diagram, expressed as a function of the temperature and of the scaled density ρR_g , should be independent on the length of the polymer at fixed number of reactive sites. The number of spacing monomers is thus irrelevant. This consideration also indicates that the (AAAA)₆ polymers will never phase separate, inde-

Name	Sequence	R_g^2/σ^2
(AAAA) ₆ (M=20)	$(AM_{20})_{23}A$	161
(ABAB) ₆ (M=20)	$(AM_{20}BM_{20})_{11}AM_{20}B$	110
(ABCD) ₆ (M=20)	$(AM_{20}BM_{20}CM_{20}DM_{20})_5AM_{20}BM_{20}CM_{20}D$	108
(AAAA) ₃ (M=20)	$(AM_{20})_{11}A$	85
(ABAB) ₃ (M=20)	$(AM_{20}BM_{20})_5AM_{20}B$	60

TABLE S2. The three polymers with larger spacing between the reactive sites.

FIG. S4. Comparison of the number of inter-polymer bonds, of the only-intra bonds effective potential βV_{eff}^{intra} , and of the effective potential βV_{eff} vs the relative distance R between the two centers of mass, rescaled by the respective gyration radii.FIG. S5. The gyration radius of single AAAA and ABAB polymers as a function of M .

pendently from the number of spacing monomers, as predicted by Semenov and Rubinstein [8].

B. Varying the degree of polymerization

We evaluate here the effect of the degree of polymerization at fixed number of spacing inert monomers ($M = 20$) on changing the number of repeating units (and hence of the reactive monomers). Specifically, polymers are constituted by 12 reactive units, for the AAAA and ABAB cases. The gyration radius of the two new polymers is also reported in Table S2. Fig. S6 compares the number of inter polymer bonds for polymers with 12 and 24 reactive sites with the same number of inert monomers. Differently from the previous case, when distances are scaled by R_g , the number of reactive site within R_g is halved. Hence, the shorter polymer has a lower probability to form inter-particle bonds, as reflected in the figure.

S3. CONFORMATIONAL AND COMBINATORIAL ENTROPIES

Figure S7 provides visual representations of the entropic contributions due to conformational and combinatorial entropies. Note that for the latter in general the different bonding patterns (see Figure S7(b)) also have different conformational contributions, since they

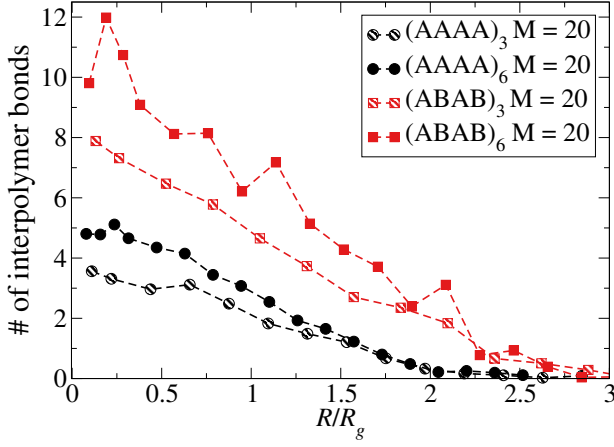


FIG. S6. Comparison of the number of inter-polymer bonds vs the relative distance between the two center of mass, scaled by the respective gyration radius.

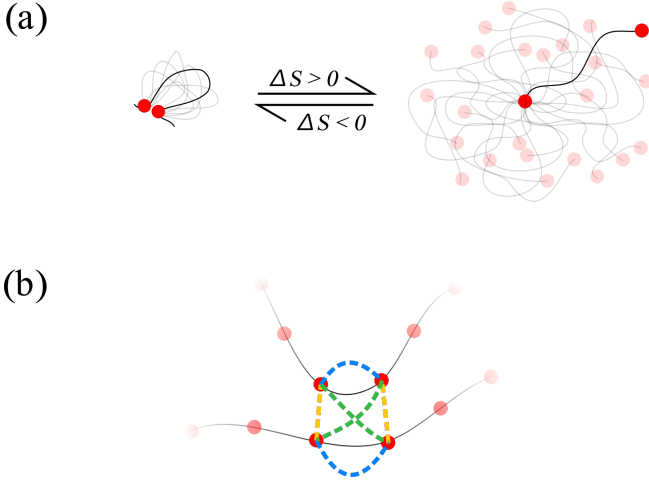


FIG. S7. Sketches providing visual representations of some of the different entropic contributions that play a role in the thermodynamics of fully-bonded SCNPs. Chains are drawn as black lines decorated with red spheres, representing the reactive monomers. The grey lines indicate possible different local configurations, one of which is highlighted in black. (a) Closing a loop costs conformational entropy, since the additional constraint greatly limits the available chain configurations (black and shaded curves). (b) In the fully-bonded limit, when sites belonging to different chains come in contact there are multiple ways of satisfying all the bonds (here shown with dotted lines). If we focus on the four attractive sites in the middle of the picture we see that there is only one possible way of forming intra-molecular bonds (blue lines), but two ways of forming inter-molecular bonds (green and yellow lines), which are thus favoured from a purely combinatorial point of view.

are composed by different numbers of inter and intra-molecular bonds. In the next section we explicitly compute the combinatorial entropy of a system composed of two polymers decorated with reactive monomers that can form both intra- and inter-molecular bonds, with the cru-

cial assumption that all bonds have the same statistical weight. For chain polymers this is a strong approximation (see *e.g.* Ref. [9]), but the derivation below can be nonetheless a useful starting point for a more rigorous approach.

S4. EVALUATING THE COMBINATORIAL ENTROPY IN A SIMPLE SYSTEM

Assume that two polymers are at a distance compatible for inter-polymer binding and that at this distance there are $2N$ reactive monomers available to form N bonds. Assume that the first N reactive monomers belong to the first polymer and that the second half belong to the second polymer. The total number of different bonding patterns is $(2N - 1)!!$ (where $!!$ indicates the double factorial), since the first picked reactive monomer can bind with $2N - 1$ other, the second picked can bind with $2N - 3$ and so on. We note that the number of states with only intra-bonds (zero inter bonds) is simply given by $[(N - 1)!!]^2$, since the first reactive monomer can bind only to $N - 1$ others and so on, generating a $(N - 1)!!$ contribution for each of the two polymers.

Thus two polymers allowed to form inter-polymer bonds are stabilized, compared to two isolated polymers in which only intra-bonds are possible by an entropic factor [10]

$$\frac{\Delta S_{\text{comb}}}{k_B} = \ln \left[\frac{(2N - 1)!!}{[(N - 1)!!]^2} \right] \quad (\text{S10})$$

If reactive monomers of different type are present, as in the ABAB and in the ABCD SCNP, the entropic difference can be generalized as

$$\frac{\Delta S_{\text{comb}}}{k_B} = \sum_{\alpha=1}^{m_t} \ln \left[\frac{(2N_{\alpha} - 1)!!}{[N_{\alpha} - 1]!!^2} \right] \quad (\text{S11})$$

where now N_{α} indicates the number of reactive sites of type α , m_t is the number of types and $N = \sum_{\alpha} N_{\alpha}$. Fig. S8 shows the resulting contribution of the combinatorial entropy S_{comb} vs N for the three different polymer topologies. ΔS_{comb} shows somewhat surprisingly a very weak dependence on topology, with a slight preference for AAAA over ABAB and ABCD within a fraction of k_B . If ΔS_{comb} were the only contribution, bonding would be just a little bit stronger for the AAAA polymer.

The limit for large N is particularly simple. It can be demonstrated by noting that the expression in Eq.(S10) can be recast by using the relations

$$(2N - 1)!! = \frac{(2N)!}{2^N N!}$$

and

$$(N - 1)!! = \frac{N!}{2^{N/2} (N/2)!}$$

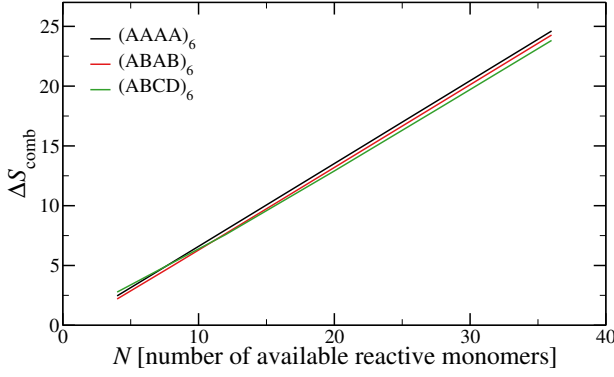


FIG. S8. Combinatorial entropic gain associated to inter-polymer binding for the three polymer configurations. All polymers are characterized by comparable entropies.

so that

$$\frac{(2N-1)!!}{[(N-1)!!]^2} = \frac{(2N)!}{N!N!} \frac{(N/2)!(N/2)!}{N!} = \frac{\binom{2N}{N}}{\binom{N}{N/2}}.$$

We now note that

$$\binom{2N}{N} = \frac{2(2N-1)}{N} \binom{2(N-1)}{N-1}.$$

By applying this relation $N/2$ times we find

$$\binom{2N}{N} = 2^{N/2} \prod_{i=0}^{N/2-1} \frac{2(N-i)-1}{N-i} \binom{N}{N/2}$$

and therefore

$$\begin{aligned} \frac{(2N(R)-1)!!}{[(N(R)-1)!!]^2} &= 2^{N/2} \prod_{i=0}^{N/2-1} \frac{2(N-i)-1}{N-i} \\ &= 2^{N/2} \prod_{i=0}^{N/2-1} 2 \left(1 - \frac{1}{2(N-i)}\right) = 2^N \prod_{i=0}^{N/2-1} \left(1 - \frac{1}{2(N-i)}\right) \end{aligned}$$

The combinatorial entropy (Eq. S10) thus can be equivalently rewritten as

$$\frac{\Delta S_{\text{comb}}}{k_B} = N \log 2 + \sum_{i=0}^{N/2-1} \log \left(1 - \frac{1}{2(N-i)}\right).$$

We can derive a simpler (approximated) expression if N is large. Indeed, in this limit $\log \left(1 - \frac{1}{2(N-i)}\right) \approx -\frac{1}{2(N-i)}$ and therefore

$$\sum_{i=0}^{N/2-1} \log \left(1 - \frac{1}{2(N-i)}\right) \approx -\frac{1}{2} \sum_{i=0}^{N/2-1} \frac{1}{N-i}$$

$$\approx -\frac{1}{2} \int_{N/2}^N \frac{dx}{x} = -\frac{1}{2} \log 2$$

so that we find

$$\frac{\Delta S_{\text{comb}}}{k_B} \approx (N - 0.5) \log 2, \quad (\text{S12})$$

simply indicating that each reactive monomer, if part of an intra bond, select half of the possible bonding possibilities.

In the general case of $m_t \neq 1$ the latter expression becomes

$$\frac{\Delta S_{\text{comb}}}{k_B} \approx (N - 0.5m_t) \log 2 \approx N \log 2.$$

In other words, in the large- N limit the combinatorial entropic attraction $\Delta S_{\text{comb}}/k_B$ does not depend on the types of reactive monomers decorating the polymer chain but only on their total number.

-
- [1] K. Kremer and G. S. Grest, The Journal of Chemical Physics **92**, 5057 (1990).
 - [2] F. H. Stillinger and T. A. Weber, Physical review B **31**, 5262 (1985).
 - [3] F. Sciortino, The European Physical Journal E **40**, 3 (2017).
 - [4] A. M. Ferrenberg and R. H. Swendsen, Computers in Physics **3**, 101 (1989).
 - [5] J. Russo, P. Tartaglia, and F. Sciortino, The Journal of Chemical Physics **131**, 014504 (2009).
 - [6] A. J. Moreno, P. Bacova, F. L. Verso, A. Arbe,

- J. Colmenero, and J. A. Pomposo, Journal of Physics: Condensed Matter **30**, 034001 (2017).
- [7] M. Formanek and A. J. Moreno, Soft Matter **13**, 6430 (2017).
- [8] A. N. Semenov and M. Rubinstein, Macromolecules **31**, 1373 (1998).
- [9] E. Zumbro, J. Witten, and A. Alexander-Katz, Biophysical Journal **117**, 892 (2019).
- [10] F. Sciortino, Y. Zhang, O. Gang, and S. K. Kumar, ACS nano **14**, 5628 (2020).